Klein Lecture Notes for 2019 GPAP School on Plasma Physics for Astrophysicists

Kristopher G. Klein

Department of Planetary Sciences, University of Arizona, Tucson, AZ 85719, USA

Lunar and Planetary Laboratory, University of Arizona, Tucson, AZ 85719, USA

(compiled on 18 June 2019)

Herein are lecture notes for portions of the 2019 GPAP School on plasma physics for astrophysicists held at Swarthmore College, June 18 to 20.

CONTENTS

PART I

Linear Theory of MHD Waves: Alfvén, Fast, and Slow modes

I.1. Linearization of the MHD Equations

One means of characterizing a plasma is by studying the *linear modes* the system supports. Such modes are driven by an initial small amplitude perturbation. The technique of calculating a linear dispersion relation that describes such modes is a very general one, and is frequently applied to many different plasma and astrophysical systems. In this lecture, we will demonstrate its application to the ideal MHD system of equations.

General Procedure for Calculating Linear Dispersion Relation

Regardless of the system in question, the same procedure is followed:

- Linearization of Equations
- Fourier Transform of $\mathcal{O}(\epsilon^1)$ Expressions
- Construction of Determinant from Fourier Expressions

Let's start with a reminder of the *ideal* MHD system of equations:

The Continuity Equation:

$$\frac{\partial \rho}{\partial t} + \nabla \cdot (\rho \boldsymbol{U}) = 0 \tag{I.1}$$

The Momentum Equation:

$$\rho \left(\frac{\partial}{\partial t} + \boldsymbol{U} \cdot \nabla \right) \boldsymbol{U} = -\nabla \left(p + \frac{B^2}{8\pi} \right) + \frac{\boldsymbol{B} \cdot \nabla \boldsymbol{B}}{4\pi} \tag{I.2}$$

The Induction Equation:

$$\frac{\partial \boldsymbol{B}}{\partial t} = \nabla \times (\boldsymbol{U} \times \boldsymbol{B}) \tag{I.3}$$

The Equation of State:

$$\frac{d}{dt} \left(p \rho^{-\gamma} \right) = 0 \rightarrow \frac{\partial p}{\partial t} + \nabla \cdot (\gamma p \boldsymbol{U}) = 0 \tag{I.4}$$

I.1.1. *Calculation of the MHD Linear Dispersion Relation*

To linearize this system, we assume each quantity can be written as background value combined with a small amplitude perturbation.

$$\rho = \rho_0 + \epsilon \delta \rho \tag{I.5}$$
$$\boldsymbol{B} = \boldsymbol{B}_0 + \epsilon \delta \boldsymbol{B} \tag{I.6}$$
$$\boldsymbol{U} = \epsilon \delta \boldsymbol{U} \tag{I.7}$$
$$p = p_0 + \epsilon \delta p \tag{I.8}$$
$$\tag{I.9}$$

where ϵ is a small ordering parameters ($\epsilon \ll 1$)[1]. We have assumed for simplicity there is no mean flow ($\boldsymbol{U}_0 = 0$) and will assume that the equilibrium quantities $\boldsymbol{B}_0$, ρ_0, and p_0 are uniform in space and stationary in time (i.e. $\nabla \cdot \boldsymbol{B}_0 = 0$ and $\partial_t \boldsymbol{B}_0 = 0$).

We now insert these expressions into Eqns I.1-I.4, and separate into $\mathcal{O}(\epsilon^0)$, $\mathcal{O}(\epsilon^1)$,

[1]For more details on asymptotic and perturbative methods, see the excellent reference Bender & Orszag (1978).

and higher order equations. The $\mathcal{O}(\epsilon^0)$ expressions describe the plasma equilibrium. To calculate the linear behavior, we retain only the $\mathcal{O}(\epsilon)$ expressions[2]:

$$\frac{\partial \delta\rho}{\partial t} = -\rho_0 \nabla \cdot \delta \boldsymbol{U} \tag{I.10}$$

$$\rho_0 \frac{\partial \delta \boldsymbol{U}}{\partial t} = -\nabla \left(\delta p + \frac{\boldsymbol{B}_o \cdot \delta \boldsymbol{B}}{8\pi} \right) + \frac{\boldsymbol{B}_0 \cdot \nabla \delta \boldsymbol{B}}{4\pi} \tag{I.11}$$

$$\frac{\partial \delta \boldsymbol{B}}{\partial t} = -\boldsymbol{B}_0 \nabla \cdot \delta \boldsymbol{U} + \boldsymbol{B}_0 \cdot \nabla \delta \boldsymbol{U} \tag{I.12}$$

$$\frac{\partial \delta p}{\partial t} = -\gamma p_0 \nabla \cdot \delta \boldsymbol{U} \tag{I.13}$$

I.1.2. *Fourier Transform of $\mathcal{O}(\epsilon^1)$ Expressions*

Given the set of linear equations above, we next rely on the fact that any disturbance can be decomposed into a sum of plane waves

$$\rho(\boldsymbol{x}, t) = \sum_{\boldsymbol{k}} \rho(\boldsymbol{k}) \exp\left[i \left(\boldsymbol{k} \cdot \boldsymbol{x} - \omega(\boldsymbol{k}) t\right)\right] \tag{I.14}$$

where $\omega(\boldsymbol{k})$ is the normal mode frequency that will satisfy the derived dispersion relation. Because our equations are linear, a solution for arbitrary wavevector $\boldsymbol{k}$ must be independent of all other wavevectors. We can therefore calculate the dispersion relation without initially specifying a particular value for $\boldsymbol{k}$. Note that the Fourier coefficients (e.g. $\rho(\boldsymbol{k})$) are complex quantities, and that to calculate an associated observable quantity, we must select the real component of the coefficient, $\mathcal{R}\left\{\rho(\boldsymbol{k}) \exp\left[i \left(\boldsymbol{k} \cdot \boldsymbol{x} - \omega(\boldsymbol{k}) t\right)\right]\right\}$.

Given this Fourier decomposition, we will take advantage of properties related to changes in space and time:

$$\frac{\partial}{\partial t}\rho(\boldsymbol{x}, t) = \rho(\boldsymbol{k}) \frac{\partial}{\partial t} \exp\left[i \left(\boldsymbol{k} \cdot \boldsymbol{x} - \omega(\boldsymbol{k}) t\right)\right] = -i\omega(\boldsymbol{k}) \rho(\boldsymbol{x}, t) \tag{I.15}$$

$$\nabla \rho(\boldsymbol{x}, t) = i\boldsymbol{k} \rho(\boldsymbol{k}) \exp\left[i \left(\boldsymbol{k} \cdot \boldsymbol{x} - \omega(\boldsymbol{k}) t\right)\right] = i\boldsymbol{k} \rho(\boldsymbol{x}, t) \tag{I.16}$$

or in shorthand:

$$\frac{\partial}{\partial t} \rightarrow -i\omega \; ; \; \nabla \rightarrow i\boldsymbol{k}. \tag{I.17}$$

Given this formalism, we can Fourier Transform our linearized equations, Eqn. I.10-I.13 into:

$$\omega \delta\rho = \rho_0 \left(\boldsymbol{k} \cdot \delta \boldsymbol{U}\right) \tag{I.18}$$

$$\omega \delta \boldsymbol{U} = \boldsymbol{k} \left(\frac{\delta p}{\rho_0} + \frac{\boldsymbol{B}_0 \cdot \delta \boldsymbol{B}}{4\pi\rho_0} \right) - \frac{\left(\boldsymbol{B}_0 \cdot \boldsymbol{k}\right) \delta \boldsymbol{B}}{4\pi\rho_0} \tag{I.19}$$

$$\omega \delta \boldsymbol{B} = \boldsymbol{B}_0 \left(\boldsymbol{k} \cdot \delta \boldsymbol{U}\right) - \left(\boldsymbol{B}_0 \cdot \boldsymbol{k}\right) \delta \boldsymbol{U} \tag{I.20}$$

$$\omega \delta p = \gamma p_0 \left(\boldsymbol{k} \cdot \delta \boldsymbol{U}\right). \tag{I.21}$$

[2]See page 4 of the NRL plasma formulary for the vector identities used in the construction of these expressions.

I.1.3. *Construction of Determinant from Fourier Expressions*

We now reduce Eqns I.18-I.21 into a single expression, the MHD dispersion relation. We first eliminate δp from Eqn.I.19 using the Equation of State, Eqn. I.21

$$\omega^2 \delta \boldsymbol{U} = \boldsymbol{k}\left(\frac{\gamma p_0 \left(\boldsymbol{k}\cdot\delta\boldsymbol{U}\right)}{\rho_0} + \frac{\boldsymbol{B}_0\cdot\left(\omega\delta\boldsymbol{B}\right)}{4\pi\rho_0}\right) - \frac{\left(\boldsymbol{B}_0\cdot\boldsymbol{k}\right)\left(\omega\delta\boldsymbol{B}\right)}{4\pi\rho_0} \tag{I.22}$$

Next, the perturbed magnetic field is eliminated by use of the induction equation, Eqn. I.20

$$\begin{aligned}\omega^2\delta\boldsymbol{U} =& \boldsymbol{k}\left(\boldsymbol{k}\cdot\delta\boldsymbol{U}\right)\left(\frac{\gamma p_0}{\rho_0}+\frac{B_0^2}{4\pi\rho_0}\right) - \boldsymbol{k}\frac{\left(\hat{\boldsymbol{b}}\cdot\delta\boldsymbol{U}\right)\left(\hat{\boldsymbol{b}}\cdot\boldsymbol{k}\right)B_0^2}{4\pi\rho_0} \\ &-\frac{B_0^2}{4\pi\rho_0}\left(\hat{\boldsymbol{b}}\cdot\boldsymbol{k}\right)\left(\boldsymbol{k}\cdot\delta\boldsymbol{U}\right)\hat{\boldsymbol{b}} + \frac{B_0^2\left(\hat{\boldsymbol{b}}\cdot\boldsymbol{k}\right)^2\delta\boldsymbol{U}}{4\pi\rho_0}\end{aligned} \tag{I.23}$$

This can be simplified further with the introduction of two characteristic speeds, the sound speed

$$c_s^2 = \frac{\gamma p_0}{\rho_0} \tag{I.24}$$

and the Alfvén speed

$$v_A^2 = \frac{B_0^2}{4\pi\rho_0}. \tag{I.25}$$

We also define, without loss of generality, the orientation of the wavevector with respect to the background magnetic field as

$$\boldsymbol{k} = k_\perp\hat{\boldsymbol{x}} + k_\parallel\hat{\boldsymbol{z}} = k\sin\theta\hat{\boldsymbol{x}} + k\cos\theta\hat{\boldsymbol{z}}. \tag{I.26}$$

Thus, we will take advantage of

$$\boldsymbol{k}\cdot\delta\boldsymbol{U} = k_\perp\delta U_x + k_\parallel\delta U_z \tag{I.27}$$

$$\boldsymbol{k}\cdot\hat{\boldsymbol{b}} = k\cos\theta \tag{I.28}$$

$$\delta\boldsymbol{U}\cdot\hat{\boldsymbol{b}} = \delta U_z \tag{I.29}$$

and write

$$\begin{aligned}\omega^2\delta\boldsymbol{U} =& \boldsymbol{k}\left(k_\perp\delta U_x + k_\parallel\delta U_z\right)\left(c_s^2+v_A^2\right) - \boldsymbol{k}v_A^2\delta U_z k_\parallel \\ &- v_A^2 k_\parallel\left(k_\perp\delta U_x + k_\parallel\delta U_z\right)\hat{\boldsymbol{b}} + v_A^2k_\parallel^2\delta\boldsymbol{U}\end{aligned} \tag{I.30}$$

Breaking this into components, we can write the 3×3 matrix expression

$$\begin{pmatrix} \omega^2 - c_s^2k_\perp^2 - v_A^2k^2 & 0 & -c_s^2k_\parallel k_\perp \\ 0 & \omega^2 - k_\parallel^2v_A^2 & 0 \\ -c_s^2k_\parallel k_\perp & 0 & \omega^2 - k_\parallel^2c_s^2 \end{pmatrix}\begin{pmatrix}\delta U_x\\ \delta U_y\\ \delta U_z\end{pmatrix} = 0 \tag{I.31}$$

whose determinant produces the dispersion relation

$$\left(\omega^2 - k_\parallel^2v_A^2\right)\left[\omega^4 - \omega^2k^2\left(c_s^2+v_A^2\right) + k_\parallel^4c_s^2v_A^2\right] = 0. \tag{I.32}$$

One can make this expression dimensionless by normalizing by kv_A (with $\bar{\omega} = \omega/kv_A$), and defining the ratio of thermal to magnetic pressure as $\beta = c_s^2/v_A^2$, producing

$$\left(\bar{\omega}^2 - \cos^2\theta\right)\left[\bar{\omega}^4 - \bar{\omega}^2\left(1+\beta\right) + \beta\cos^2\theta\right] = 0. \tag{I.33}$$

This equation has three kinds of normal mode solutions, namely **Alfvén** waves, which

are the solutions to $\omega^2 - k_\parallel^2 v_A^2 = 0$ and **Fast** and **Slow** magnetosonic waves, which are solutions to $\omega^4 - \omega^2 k^2 \left(c_s^2 + v_A^2\right) + k_\parallel^4 c_s^2 v_A^2 = 0$.[3] The behavior of these waves as a function of the pressure ratio β and the wavevector angle θ are discussed next.

I.2. MHD Waves and Their Properties

We next detail the behavior of these normal mode solutions. We start with the consideration of the limiting cases of $\theta = 0$ ($\boldsymbol{k}$ and $\hat{\boldsymbol{b}}$ aligned) and $\theta = \pi/2$ ($\boldsymbol{k}$ perpendicular to $\hat{\boldsymbol{b}}$), before exploring the general θ case.

I.2.1. *Parallel Wavevectors:* $\theta = 0$

When $\boldsymbol{k}$ and $\hat{\boldsymbol{b}}$ are aligned, the dispersion tensor reduces to

$$\begin{pmatrix} \omega^2 - k_\parallel^2 v_A^2 & 0 & 0 \\ 0 & \omega^2 - k_\parallel^2 v_A^2 & 0 \\ 0 & 0 & \omega^2 - k_\parallel^2 c_s^2 \end{pmatrix} \begin{pmatrix} \delta U_x \\ \delta U_y \\ \delta U_z \end{pmatrix} = 0 \tag{I.34}$$

or equivalently the determinant Eqn. I.32 simplifies to

$$\left(\omega^2 - k_\parallel^2 v_A^2\right) \left[\omega^4 - \omega^2 k_\parallel^2 \left(c_s^2 + v_A^2\right) + k_\parallel^4 c_s^2 v_A^2\right] = 0 \tag{I.35}$$

$$\left(\omega^2 - k_\parallel^2 v_A^2\right)^2 \left(\omega^2 - k_\parallel^2 c_s^2\right) = 0. \tag{I.36}$$

There are six solutions to this dispersion relation: $\omega = \pm k_\parallel v_A$ (one for $U_x \neq 0, U_y = 0$, one pair for $U_x = 0, U_y \neq 0$), and $\omega = \pm k_\parallel c_s$. The former is the Alfvén wave, the later the sound wave.

The Alfvén wave is polarized transverse to $\boldsymbol{B}_0$ and propagates along $\boldsymbol{B}_0$, like waves on a string. For the case of $U_x \neq 0$, let's look at the $\hat{x}$ components of the momentum equation

$$\frac{\partial \delta U_x}{\partial t} = \frac{B_0}{4\pi\rho_0} \frac{\partial \delta B_x}{\partial z} \tag{I.37}$$

and the induction equation

$$\frac{\partial \delta B_x}{\partial t} = B_0 \frac{\partial \delta U_x}{\partial z}. \tag{I.38}$$

For the Alfvén wave, a velocity perturbation perpendicular to $\boldsymbol{B}_0$ bends the magnetic field. The magnetic tension ($\frac{B_0}{4\pi\rho_0} \frac{\partial \delta B_x}{\partial z}$) acts as a restoring force, driving the wave motion that propagates at the Alfvén speed v_A.

Note that because $\boldsymbol{k} \cdot \boldsymbol{U} = 0$ the motion of the Alfvén wave is incompressible. This is different than the sound wave, which arises for $\delta U_z \neq 0$. In this case, the relevant equations driving the behavior of the wave are the $\hat{z}$ component of the momentum equation

$$\rho_0 \frac{\partial \delta U_z}{\partial t} = -\frac{\partial \delta p}{\partial z} \tag{I.39}$$

[3] There is also an **Entropy mode**, corresponding to a relabeling of fluid elements that allows for fluctuations in entropy while enforcing constant pressure, that was removed from our dispersion relation when we included our equation of state.

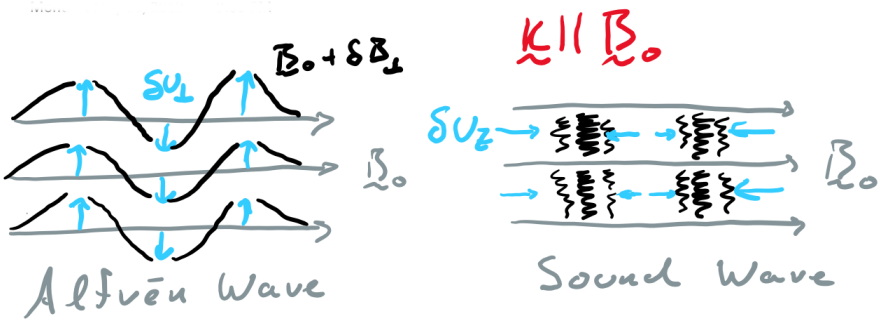

FIGURE 1. Schematic of the Alfvén and sound waves that occur for $\boldsymbol{k} \parallel \boldsymbol{B}_0$.

and the pressure equation:

$$\frac{\partial \delta p}{\partial t} = -\gamma p_0 \frac{\partial \delta U_z}{\partial z}. \tag{I.40}$$

The parallel motion along $\boldsymbol{B}_0$, δU_z, leads to compression; pressure acts as a restoring force; this is the same as the typical sound wave that moves through a gas.

I.2.2. *Perpendicular Wavevectors:* $\theta = \pi/2$

When $\boldsymbol{k}$ is normal to $\hat{\boldsymbol{b}}$, the dispersion tensor reduces to

$$\begin{pmatrix} \omega^2 - k_\perp^2 \left(c_s^2 + v_A^2\right) & 0 & 0 \\ 0 & \omega^2 & 0 \\ 0 & 0 & \omega^2 \end{pmatrix} \begin{pmatrix} \delta U_x \\ \delta U_y \\ \delta U_z \end{pmatrix} = 0 \tag{I.41}$$

of equivalently the determinant Eqn. I.32 simplifies to

$$\omega^4 \left[\omega^2 - k_\perp^2 \left(c_s^2 + v_A^2\right)\right]^2 = 0. \tag{I.42}$$

As with the $\theta = 0$ case, there are six solutions. Four solutions have $\omega = 0$ and two satisfy $\omega = \pm k_\perp \left(c_s^2 + v_A^2\right)^{1/2}$. For $\delta U_z \neq 0$, there is motion along the magnetic field, but the motion is incompressible ($\boldsymbol{k} \cdot \boldsymbol{U} = 0$). For $\delta U_y \neq 0$, the motion is normal to the $(\boldsymbol{B}_0, \boldsymbol{k})$ plane, so fields simply slide past one another (this is known as interchange motion). In both cases, there is no restoring force to the perturbed velocities, and thus there is no wave motion (i.e. $\omega = 0$).

For $\delta U_x \neq 0$ case, we have a magneto-acoustic (or fast) wave. The motion is driven by compressions, like the sound wave, but with the help of the magnetic field. Let's look at the relevant components of the momentum equation

$$\frac{\partial \delta U_x}{\partial t} = -\frac{\partial}{\partial x}\left(\frac{\delta p}{\rho_0} + \frac{B_0}{4\pi\rho_0}\delta B_z\right), \tag{I.43}$$

the induction equation

$$\frac{\partial \delta B_z}{\partial t} = -B_0 \frac{\partial \delta U_x}{\partial x}, \tag{I.44}$$

and the pressure equation

$$\frac{\partial \delta p}{\partial t} = -\gamma p_0 \frac{\partial \delta U_x}{\partial x}. \tag{I.45}$$

The perpendicular perturbation δU_x compresses both the plasma and the magnetic field, and the thermal and magnetic pressure act in concert as a restoring force.

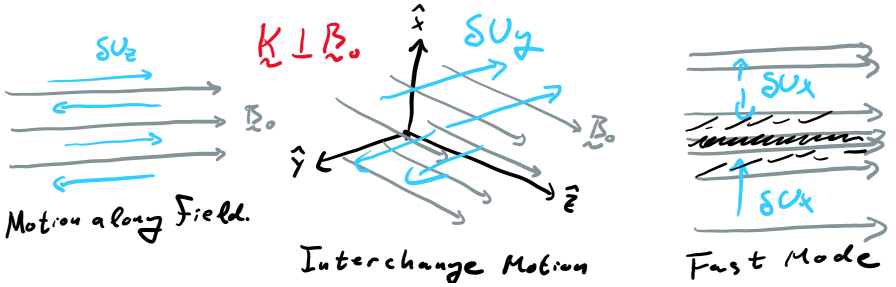

FIGURE 2. Schematic of the normal modes that occur for $\boldsymbol{k} \perp \boldsymbol{B}_0$.

I.2.3. *Wave Eigenfunctions for MHD Eigenmodes*

Before turning to the general solution, we should step back and ask, given a particular normal mode for our system $\omega(\boldsymbol{k})$, how do the perturbed quantities respond? We have discussed this somewhat vaguely above; let's now attempt a bit more rigorous approach.

The process for determining the eigenfunctions is as follows:

- Derive a set of linear equations (we have thankfully already done this).
- Select a value for one component of an eigenfunction (e.g. $\delta U_x = U_0$)
- Solve for the other desired quantities in terms of U_0.

This process can involve *some* linear algebra, which won't be covered in detail here, but will be left as an exercise for the reader.

One of the nice aspects of the form of Eqn I.31 is that δU_y is decoupled from δU_x and δU_z. This makes solving for the Alfvén eigenfunctions quite simple, and the fast and slow modes *less* complicated.

I.2.4. *General Wavevector Solution*

I.2.4.1. *Alfvén Waves*

As with the $\theta = 0$ case, we can simply write the Alfvén dispersion relation by inspection of Eqn.I.32; $\omega = \pm k_\parallel v_A$. All motion of these waves are in the $\hat{y}$ direction. Thus $\boldsymbol{k} \cdot \boldsymbol{U} = 0$ (the waves are incompressible), which means there are no density or pressure fluctuations associated with Alfvén waves.

Returning to Eqn. I.20, we can quantify the relation between the magnetic and velocity fluctuations:

$$\omega \delta \boldsymbol{B} = \boldsymbol{B}_0 \left(\boldsymbol{k} \cdot \delta \boldsymbol{U}\right) - \left(\boldsymbol{B}_0 \cdot \boldsymbol{k}\right) \delta \boldsymbol{U} \tag{I.46}$$

$$\omega \delta B_y = B_0 k_\parallel \delta U_y \rightarrow -\frac{\delta B_y}{B_0} = -\frac{k_\parallel}{\omega} \delta U_y = \mp \frac{\delta U_y}{v_A} \tag{I.47}$$

As discussed previously, the only restoring force associated with this wave motion is the magnetic tension. A schematic of Alfvén waves is shown in Fig. 3. This Alfvénic in phase or π out of phase relation between $\delta \boldsymbol{B}$ and $\delta \boldsymbol{U}$ is seen in many plasma systems; a particular example from the solar wind is Belcher & Davis (1971).

I.2.4.2. *Fast and Slow Waves*

The general fast and slow wave dispersion relation, solving the non-Alfvénic component of Eqn I.33, is

$$\bar{\omega}^2 = \frac{1 + \beta \pm \sqrt{\left(1 + \beta\right)^2 - 4\beta \cos^2 \theta}}{2} \tag{I.48}$$

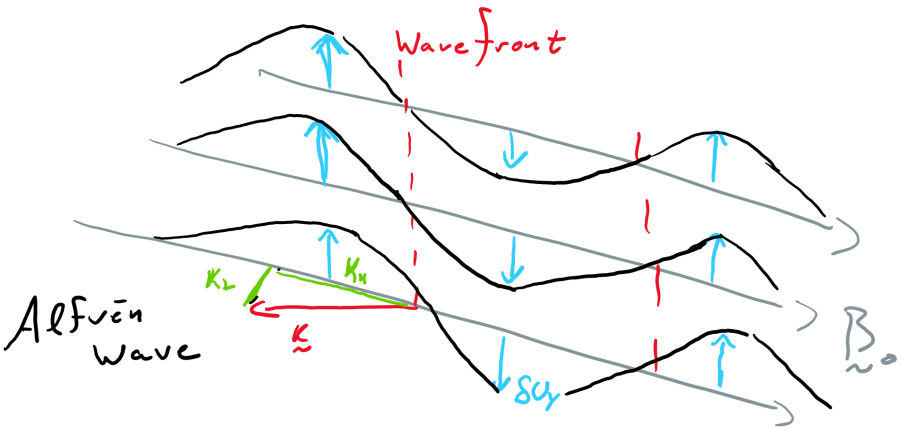

FIGURE 3. Schematic of the Alfvén mode for an arbitrary $\boldsymbol{k}$.

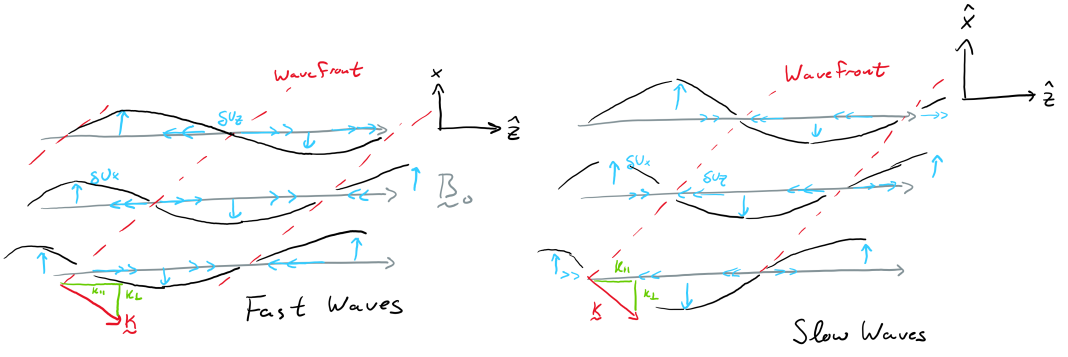

FIGURE 4. Schematic of the Fast and Slow modes for arbitrary $\boldsymbol{k}$.

where the positive (negative) root is the fast (slow) solution. Schematics of these waves are presented in Fig. 4.

The wave motion associated with both of these modes is entirely in the $\hat{x} - \hat{z}$ plane, and unlike the Alfvén mode, is generally compressible ($\boldsymbol{k} \cdot \boldsymbol{U} \neq 0$). To understand the behavior of these waves, let's take a look at the $\hat{x}$ & $\hat{z}$ components of Eqn. I.31

$$\begin{pmatrix} \omega^2 - c_s^2 k_\perp^2 - v_A^2 k^2 & -c_s^2 k_\parallel k_\perp \\ -c_s^2 k_\parallel k_\perp & \omega^2 - k_\parallel^2 c_s^2 \end{pmatrix} \begin{pmatrix} \delta U_x \\ \delta U_z \end{pmatrix} = 0 \tag{I.49}$$

Using either of these equations, we can solve for δU_z in terms of δU_x

$$\delta U_z = \frac{c_s^2 k_\parallel k_\perp}{\omega^2 - k_\parallel^2 c_s^2} \delta U_x. \tag{I.50}$$

This expression, combined with Eqn I.18, allows us to determine the density response

$$\delta \rho = \frac{\omega \rho_0 k_\perp}{\omega^2 - k_\parallel^2 c_s^2} \delta U_x. \tag{I.51}$$

Similarly, using Eqn. I.20, we can write the magnetic field eigenfunctions for the fast

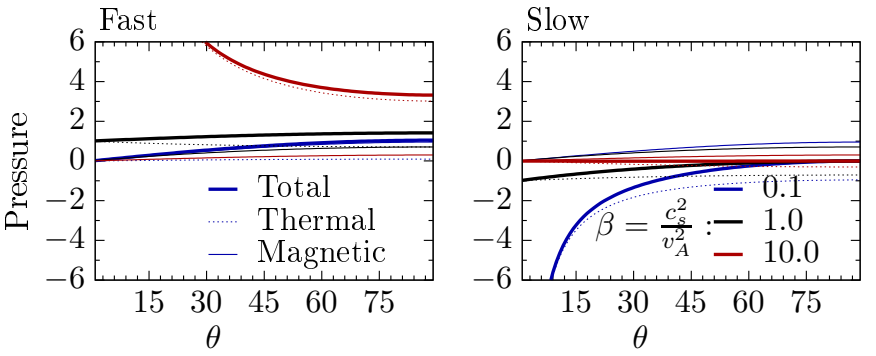

FIGURE 5. Comparison of the total, thermal, and magnetic pressures for the Fast and Slow modes as a function of angle and β.

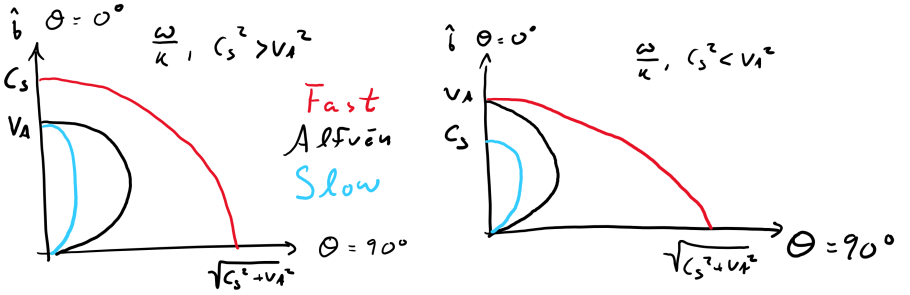

FIGURE 6. Polar plot of the wave phase speed ω/k for the **Alfvén**, fast, and slow waves for high-β ($c_s^2 > v_A^2$) and low-β ($c_s^2 < v_A^2$).

and slow waves

$$\delta B_x = -\frac{B_0 k_\perp}{\omega}\delta U_x \tag{I.52}$$

$$\delta B_z = \frac{B_0 k_\perp}{\omega}\delta U_x. \tag{I.53}$$

What does this mean for the pressure that drives the motion of these waves? The linearized thermal and magnetic pressure (see the first term on the right hand side of Eqn. I.19) can be written as

$$\left(\frac{\delta p}{\rho_0} + \frac{\boldsymbol{B}_0 \cdot \delta \boldsymbol{B}}{4\pi\rho_0}\right) = \frac{k_\perp \delta U_x}{\omega}\left(c_s^2 \frac{\omega^2}{\omega^2 - k_\parallel c_s^2} + v_A^2\right) = \frac{\sin\theta \delta U_x}{\bar{\omega} v_A}\left(\beta \frac{\bar{\omega}^2}{\bar{\omega}^2 - \cos^2\theta\beta} + 1\right) \tag{I.54}$$

A numerical evaluation of the thermal, magnetic, and total pressure is presented in Fig. 5.

Careful evaluation of this term reveals that for the fast mode solution, the thermal and magnetic pressure terms always add together, producing a strong restoring force and a faster wave. For perpendicular angles $\theta = \pi/2$, the fast mode becomes the previously discussed magnetosonic wave. At small angles, the fast mode becomes either the sound wave in the high-β limit or the Alfvén wave in the low-β limit.

For the slow mode solution, the two pressure terms oppose one another, leading to a weaker restoring force and a slower wave; for $\theta \to \pi/2$, the pressures completely cancel one another, suppressing wave motion. At small angles, the slow mode becomes either the Alfvén wave in the high-β limit or the sound wave in the low-β limit.

The general solutions to Eqn.I.32 can be illustrated using a Fredrick's diagram, shown for low and high β cases in Fig. 6.

Takeaway Points:

- Linearization is a useful general method for studying systems of equations.
- Ideal MHD has three characteristic waves, the Alfvén, fast, and slow mode, as well as a non-propagating entropy mode.
- The orientation of the local magnetic field to the wavevector, θ, and the ratio of the thermal to magnetic pressure, β, parameterize the behavior of the MHD normal modes.

PART II

Introduction to Kinetic Theory: Klimontovich, Vlasov, and Landau

II.1. What if collisions aren't strong enough?

We have thus far mostly focused on single particle motion, or on systems in which the physics can be adequately described by a (magneto) fluid. What happens when the collisions that enforce a fluid-like behavior are not strong enough? Must in these cases we revert to tracking the motion of each particle?

Unfortunately, there are simply too many particles to track each individually, and thus we must construct a statistical description for the ensemble of particles. This process of moving from a self consistent description of each and every particle, called the *Klimontovich Equation*, through a process called the BBGKY hierarchy (after work by Bogoliubov, Born, Green, Kirkwood, and Yvon) which involves ensemble averaging of the individual particles into a phase-space distribution, to a more tractable system is too involved a topic for the time available. For those interested, most standard graduate level texts have an in depth description (the presentation in Nicholson (1983) is particularly lucid).

Instead, we introduce the distribution function $f_s(\boldsymbol{x}, \boldsymbol{v}, t)$. $d^3\boldsymbol{x}d^3\boldsymbol{v}f_s(\boldsymbol{x}, \boldsymbol{v}, t)$ is the number of particles of species s in the 6D phase-space volume defined by $\Delta\boldsymbol{x}\Delta\boldsymbol{v}$. From this intuitive picture, f_s is a number density in phase space. Where there are no collisions, particles at nearby points move together in a fashion analogous to an incompressible 6D fluid. Taking velocity moments of f_s yields useful quantities, such as the density of species s (the zeroth moment),

$$n_s(\boldsymbol{x}, t) = \int d^3\boldsymbol{v} f_s(\boldsymbol{x}, \boldsymbol{v}, t), \tag{II.1}$$

the fluid velocity (the first moment),

$$\boldsymbol{U}_s(\boldsymbol{x}, t) = \frac{1}{n_s(\boldsymbol{x}, t)} \int d^3\boldsymbol{v}\boldsymbol{v} f_s(\boldsymbol{x}, \boldsymbol{v}, t), \tag{II.2}$$

the kinetic energy density (the second moment)

$$\mathcal{E}_s(\boldsymbol{x}, t) = \int d^3\boldsymbol{v} \frac{m_s v^2}{2} f_s(\boldsymbol{x}, \boldsymbol{v}, t), \tag{II.3}$$

etc. We will investigate the governing equations for f_s, and look into a quintessential kinetic process, Landau damping.

II.2. The Vlasov Equation

From the BBGKY hierarchy, one can derive a description for the dynamic behavior of the phase-space density (our distribution function f_s). This description takes the form of the Boltzmann (or Vlasov-Landau) equation:

$$\frac{\partial f_s}{\partial t} + \boldsymbol{v} \cdot \nabla f_s + \frac{q_s}{m_s}\left(\boldsymbol{E} + \frac{\boldsymbol{v} \times \boldsymbol{B}}{c}\right) \cdot \frac{f_s}{\partial \boldsymbol{v}} = \left(\frac{\partial f_s}{\partial t}\right)_c \tag{II.4}$$

$f_s(\boldsymbol{x}, \boldsymbol{v}, t)$ is the distribution function of species s. The Vlasov-Landau equation is

closed by the Maxwell equations

$$\nabla \cdot \boldsymbol{E} = 4\pi \sum_s q_s \int d^3\boldsymbol{v} f_s(\boldsymbol{x}, \boldsymbol{v}, t) \tag{II.5}$$

$$\nabla \cdot \boldsymbol{B} = 0 \tag{II.6}$$

$$\nabla \times \boldsymbol{E} = -\frac{1}{c}\frac{\partial \boldsymbol{B}}{\partial t} \tag{II.7}$$

$$\nabla \times \boldsymbol{B} = \frac{1}{c}\frac{\partial \boldsymbol{E}}{\partial t} + \frac{4\pi}{c}\sum_s q_s \int d^3\boldsymbol{v}\boldsymbol{v} f_s(\boldsymbol{x}, \boldsymbol{v}, t) \tag{II.8}$$

$$\tag{II.9}$$

The Landau collision operator $\left(\frac{\partial f_s}{\partial t}\right)_c$ depends on the distribution of species s as well as with all other species s'. Without going into gory details, we simply note that the collision operator has the following properties:

$$\int d^3\boldsymbol{v} \left(\frac{\partial f_s}{\partial t}\right)_c = 0 \text{ Conserves individual species particle number} \tag{II.10}$$

$$\sum_s \int d^3\boldsymbol{v} m_s \boldsymbol{v} \left(\frac{\partial f_s}{\partial t}\right)_c = 0 \text{ Conserves total momentum} \tag{II.11}$$

$$\sum_s \int d^3\boldsymbol{v} \frac{m_s v^2}{2} \left(\frac{\partial f_s}{\partial t}\right)_c = 0 \text{ Conserves total energy} \tag{II.12}$$

$$\frac{d}{dt}\left[-\sum_s \int d^3\boldsymbol{x} \int d^3\boldsymbol{v} f_s \ln f_s\right] = -\sum_s \int d^3\boldsymbol{x} \int d^3\boldsymbol{v} \left(\frac{\partial f_s}{\partial t}\right)_c \ln f_s \geqslant 0 \text{ Boltzmann's H theorem} \tag{II.13}$$

$$\left(\frac{\partial f_s}{\partial t}\right)_c \text{ removes small-scale structure in velocity space through diffusion.} \tag{II.14}$$

For these notes, we will assume that the system is non-relativistic ($v^2/c^2 \ll 1$) and quasi-neutral ($\sum_s q_s n_s = 0$). Expressions similar to those presented earlier in this school can be derived by taking moments of Eqn.II.4. The evolution of each moment will depend on the next higher term (n_s on $\boldsymbol{u}_s$, $\boldsymbol{u}_s$ on $\underline{\underline{P}}_s$...), so some choice of how to close your system of moment equations needs to be concocted and justified.

II.3. Landau Damping

So, why do we go to all this trouble to work with f_s when fluid equations seems to provide a decent description of a plasma system? The short answer is that there are some phenomena in a kinetic system that can not be properly captured when the system is reduced to being a function of solely position. The quintessential example of such a phenomenon is Landau damping, the collisionless damping of electrostatic waves via wave-particle resonances. In a fluid, the large rate of collisions prevents any resonant behavior. Most plasma textbooks will have a discussion of Landau damping; if one doesn't, the book might not be worth your time.

Before we dive into the maths, an overview of the physics of Landau damping. Consider an electrostatic wave with wavenumber $k = 2\pi/\lambda$ and frequency ω. For a velocity

distribution that has a negative velocity gradient $\partial f_s/\partial v < 0$ at the resonant velocity $v = \omega/k$, there are more particles just slower that ω/k than there are those slightly faster than ω/k. The slower particles are accelerated by the electric field seen in their reference frame, while the faster particles are decelerated. As there are more slow particles than fast, the wave loses energy, but this energy transfer from the wave to the particles is conservative and reversible.

This process of energy transfer also forms small scale structure in velocity space due to shearing in phase-space. Eventually, the structure is fine enough that collisions begin to act, increasing entropy and smoothing out $f_s(\boldsymbol{v})$.

The traditional calculation that you will see in many texts, and the one first derived by Landau (Landau 1946), is for plasma oscillations. Here, we will consider the case of ion-acoustic waves, under the simplifying assumptions of low frequencies and quasi-neutrality.

We start with the electrostatic Vlasov Equation (with no collisions)

$$\frac{\partial f_s}{\partial t} + \boldsymbol{v}\cdot\nabla f_s - \frac{q_s}{m_s}\boldsymbol{E}\cdot\frac{\partial f_s}{\partial \boldsymbol{v}} = 0 \tag{II.15}$$

and linearize, using $f_s = F_s(\boldsymbol{v}) + \epsilon\delta f_s(\boldsymbol{x},\boldsymbol{v},t)$ and $\boldsymbol{E} = \epsilon\delta\boldsymbol{E}(\boldsymbol{x},t)$. Retained terms of $\mathcal{O}(\epsilon^1)$ produces

$$\left(\frac{\partial}{\partial t} + \boldsymbol{v}\cdot\nabla\right)\delta f_s(\boldsymbol{x},\boldsymbol{v},t) + \frac{q_s}{m_s}\delta\boldsymbol{E}\cdot\frac{\partial F_s(\boldsymbol{v})}{\partial \boldsymbol{v}} = 0. \tag{II.16}$$

To determine the evolution of the electric field perturbations, we will use quasi-neutrality

$$\sum_s q_s\delta n_s = \sum_s q_s\int d^3\boldsymbol{v}\delta f_s(\boldsymbol{x},\boldsymbol{v},t) = 0. \tag{II.17}$$

Instead of taking the well-trod path of Fourier transforming in both space and time, which was done in Vlasov (1945), the solution must be solved as an initial value problem, Fourier transforming in space while performing a Laplace transform[4] in time. These transforms are defined as [5]

$$f(\boldsymbol{k}) = \int\frac{d^3\boldsymbol{x}}{(2\pi)^3}e^{-i\boldsymbol{k}\cdot\boldsymbol{x}}f(\boldsymbol{x}) \tag{II.18}$$

$$f(\omega) = \int_0^\infty dt e^{i\omega t}f(t). \tag{II.19}$$

Under a Fourier transform in space and Laplace transform in time, Eqn. II.16 becomes

$$(-i\omega + i\boldsymbol{k}\cdot\boldsymbol{v})\,\delta f_s(\boldsymbol{k},\boldsymbol{v},\omega) - \delta f_s(\boldsymbol{k},\boldsymbol{v},t=0) + \frac{q_s}{m_s}\delta\boldsymbol{E}(\boldsymbol{k},\omega)\cdot\frac{\partial F_s(\boldsymbol{v})}{\partial\boldsymbol{v}} = 0 \tag{II.20}$$

where we have exploited the nature of the time derivative under a Laplace transform $f_s'(\omega) = -i\omega f_s(\omega) - f_s(t=0)$ where the last term is the initial value of f_s.

This can be rearranged to yield an expression for the transformed distribution function

$$\delta f_s(\boldsymbol{k},\boldsymbol{v},\omega) = \frac{\delta f_s(\boldsymbol{k},\boldsymbol{v},t=0)}{-i\,(\omega-\boldsymbol{k}\cdot\boldsymbol{v})} - \frac{q_s}{m_s}\left[\frac{\delta\boldsymbol{E}(\boldsymbol{k},\omega)\cdot\frac{\partial F_s(\boldsymbol{v})}{\partial\boldsymbol{v}}}{-i\,(\omega-\boldsymbol{k}\cdot\boldsymbol{v})}\right]. \tag{II.21}$$

[4] Some texts will use $p = -i\omega$ instead of ω for the Laplace transform. Take care in moving between sources.

[5] See the introductory section of Landau (1946) for critiques of the double Fourier method

We next need to eliminate δE. This can be done by using Eqn. II.17 and substituting in $\delta f_s(\boldsymbol{k},\boldsymbol{v},\omega)$

$$\sum_s q_s \int d^3\boldsymbol{v} \frac{\delta f_s(\boldsymbol{k},\boldsymbol{v},t=0)}{-i\left(\omega-\boldsymbol{k}\cdot\boldsymbol{v}\right)} - \sum_s \frac{q_s^2}{m_s}\delta\boldsymbol{E}(\boldsymbol{k},\omega)\cdot\int d^3\boldsymbol{v}\frac{\frac{\partial F_s(\boldsymbol{v})}{\partial \boldsymbol{v}}}{-i\left(\omega-\boldsymbol{k}\cdot\boldsymbol{v}\right)} = 0. \tag{II.22}$$

Assigning the direction of $\delta\boldsymbol{E}$ as $\parallel$, we can write

$$\delta E_\parallel(\boldsymbol{k},\omega) = \frac{\sum_s q_s \int d^3\boldsymbol{v}\frac{\delta f_s(\boldsymbol{k},\boldsymbol{v},t=0)}{-i(\omega-\boldsymbol{k}\cdot\boldsymbol{v})}}{\sum_s \frac{q_s^2}{m_s}\int \frac{\partial F_s(\boldsymbol{v})}{\partial v_\parallel}\frac{d^3\boldsymbol{v}}{-i(\omega-\boldsymbol{k}\cdot\boldsymbol{v})}}. \tag{II.23}$$

In the electrostatic case, $\delta\boldsymbol{E}(\boldsymbol{k},\omega) = -i\boldsymbol{k}\phi(\boldsymbol{k},\omega)$, allowing us to write

$$\phi(\boldsymbol{k},\omega) = \frac{4\pi}{k^2}\frac{1}{D(\boldsymbol{k},\omega)}\sum_s q_s\int d^3\boldsymbol{v}\frac{\delta f_s(\boldsymbol{k},\boldsymbol{v},t=0)}{-i\left(\omega-\boldsymbol{k}\cdot\boldsymbol{v}\right)} \tag{II.24}$$

where the dielectric function is defined as

$$D(\boldsymbol{k},\omega) = \frac{4\pi}{k^2}\sum_s \frac{q_s^2}{m_s}\int d^3\boldsymbol{v}\frac{\boldsymbol{k}\cdot\partial F_s/\partial\boldsymbol{v}}{(\omega-\boldsymbol{k}\cdot\boldsymbol{v})}. \tag{II.25}$$

Our solution for δE can be in turn substituted back into Eqn. II.21 to yield an expression for δf_s:

$$\delta f_s(\boldsymbol{k},\boldsymbol{v},\omega) = \frac{\delta f_s(\boldsymbol{k},\boldsymbol{v},t=0)}{-i\left(\omega-\boldsymbol{k}\cdot\boldsymbol{v}\right)} - \frac{q_s}{m_s}\frac{\partial F_s(\boldsymbol{v})}{\partial v_\parallel}\frac{1}{-i\left(\omega-\boldsymbol{k}\cdot\boldsymbol{v}\right)}\left[\frac{\sum_{s'} q_{s'}\int d^3\boldsymbol{v}'\frac{\delta f_{s'}(\boldsymbol{k},\boldsymbol{v}',t=0)}{-i(\omega-\boldsymbol{k}\cdot\boldsymbol{v}')}}{\sum_{s'}\frac{q_{s'}^2}{m_{s'}}\int\frac{\partial F_{s'}(\boldsymbol{v}')}{\partial v'_\parallel}\frac{d^3\boldsymbol{v}'}{-i(\omega-\boldsymbol{k}\cdot\boldsymbol{v}')}}\right] \tag{II.26}$$

In order to extract $\delta f_s(\boldsymbol{x},\boldsymbol{v},t)$ from the above, an inverse-Laplace transform will need to be performed on Eqn. II.26 of the form

$$f(t) = \int_L \frac{d\omega}{2\pi}e^{-i\omega t}f(\omega) \tag{II.27}$$

where L is the Laplace contour, a straight line in complex frequency space parallel to the real ω axis (see the left panel of Fig. 7). The contour intersects the imaginary ω axis at value σ; as long as there exists $\sigma\in\mathcal{R}\ni|f(t)|<e^{\sigma t}$ as $t\to\infty$, the Laplace transform integral exists $\forall\omega\ni\mathcal{I}(\omega)\geqslant\sigma$. (see your favorite book on complex analysis for more details (Brown & Churchill 2004)).

Hence, so the inverse transforms can be written as

$$\phi(\boldsymbol{k},t) = \int_L\frac{d\omega}{2\pi}e^{-i\omega t}\frac{4\pi}{k^2}\frac{1}{D(\boldsymbol{k},\omega)}\sum_s q_s\int d^3\boldsymbol{v}\frac{\delta f_s(\boldsymbol{k},\boldsymbol{v},t=0)}{-i\left(\omega-\boldsymbol{k}\cdot\boldsymbol{v}\right)} \tag{II.28}$$

and

$$\begin{aligned}\delta f_s(\boldsymbol{k},\boldsymbol{v},t) = &\int_L\frac{d\omega}{2\pi}e^{-i\omega t}\frac{\delta f_s(\boldsymbol{k},\boldsymbol{v},t=0)}{-i\left(\omega-\boldsymbol{k}\cdot\boldsymbol{v}\right)}\\ &-\int_L\frac{d\omega}{2\pi}e^{-i\omega t}\left\{\left[\frac{\sum_{s'}\frac{q_sq_{s'}}{m_s}\frac{\partial F_s(\boldsymbol{v})/\partial v_\parallel}{-i(\omega-\boldsymbol{k}\cdot\boldsymbol{v})}\int d^3\boldsymbol{v}'\frac{\delta f_s(\boldsymbol{k},\boldsymbol{v}',t=0)}{(\omega-\boldsymbol{k}\cdot\boldsymbol{v}')}}{\sum_{s'}\frac{q_{s'}^2}{m_s}\int\frac{\partial F_s(\boldsymbol{v}')}{\partial v'_\parallel}\frac{d^3\boldsymbol{v}'}{(\omega-\boldsymbol{k}\cdot\boldsymbol{v}')}}\right]\right\}\end{aligned} \tag{II.29}$$

To perform this integral, the Laplace contour L must be shifted to $-\infty$. However, the contour can not cross any of the poles of $\delta f_s(\boldsymbol{k},\boldsymbol{v},t)$ (e.g. $\omega=\boldsymbol{k}\cdot\boldsymbol{v}$ or at a normal mode

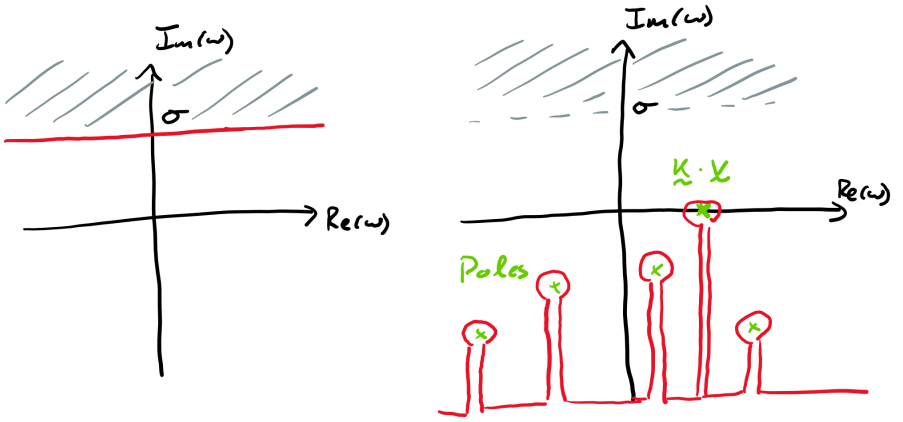

FIGURE 7. The contour used for the inverse Laplace transform (Eqn. II.27, left) as well as the deformed contour used in the specific evaluations of Eqns. II.28 and II.29.

frequency of the system). To do this, one performs an **analytic continuation** of the contour, deforming it around all of the poles of the system. This deformation is illustrated in the right hand panel of Fig. 7. Again, more details can be found in Brown & Churchill (2004) or a sufficiently advanced plasma textbook of your choosing.

This analytic continuation allows us to write the transformed quantities in the form

$$\sum_j \frac{c_j}{-i\left(\omega-\omega_k\right)} + A(\omega) \tag{II.30}$$

where ω_j are the poles of the quantity in question.

One can perform the integrals in Eqns. II.28 and II.29 through the application of Cauchy's residue theorem (complex analysis arises with suprising frequency in kinetic plasma physics; see comment about Brown & Churchill (2004) above). In performing these integrals, we find that

$$\begin{aligned}\phi(\boldsymbol{k},t) &= \int_L \frac{d\omega}{2\pi} e^{-i\omega t}\left[\sum_j \frac{c_j}{-i\left(\omega-\omega_k\right)} + A(\omega)\right] \\ &= \sum_j c_j \exp\left(-i\omega_j t\right)\end{aligned} \tag{II.31}$$

where the poles here are the zeros of $D(\boldsymbol{k},\omega)$ and those of the initial condition. The physical interpretation of the above is that $\phi(\boldsymbol{k},t)$ is the sum of a number of damped modes.

The behavior of the distribution function is slightly different. Carrying out the inverse-Laplace transform yields

$$\begin{aligned}\delta f_s(\boldsymbol{k},\boldsymbol{v},t) = &\left[\delta f_s(\boldsymbol{k},\boldsymbol{v},t=0) - \frac{q_s}{m_s} i\boldsymbol{k}\cdot\frac{\partial F_s}{\partial \boldsymbol{v}}\sum_j \frac{c_j}{-i\omega_j + i\boldsymbol{k}\cdot\boldsymbol{v}}\right]\exp\left(-i\boldsymbol{k}\cdot\boldsymbol{v}t\right) \\ &+\frac{q_s}{m_s} i\boldsymbol{k}\cdot\frac{\partial F_s}{\partial \boldsymbol{v}}\sum_j \frac{c_j \exp\left(-i\omega_j t\right)}{-i\omega_j + i\boldsymbol{k}\cdot\boldsymbol{v}}.\end{aligned} \tag{II.32}$$

What does this mean? The time-dependent behavior of the distribution function is a

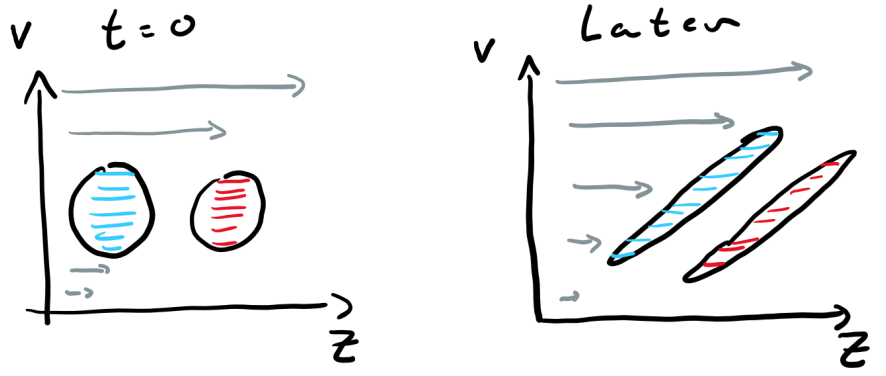

FIGURE 8. Shear

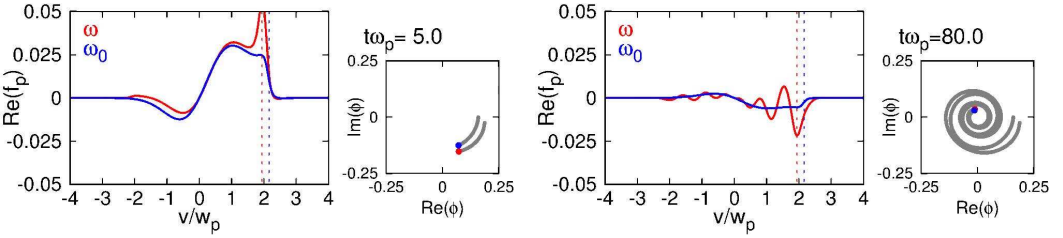

FIGURE 9. Time evolution of the Landau damping of a perturbed velocity distribution and the associated electrostatic potential. An Artificial removal of the ballistic term (blue) removes the formation of small scale velocity space structure see in the physical system (red).

combination of decaying eigenmode solutions and a *ballistic response* (the $\exp(-i\boldsymbol{k}\cdot\boldsymbol{v}t)$ terms) which oscillate without decaying.

So, we have a potential that decays with time, and a particle distribution that has decaying and non-decaying terms; these terms act in concert to conserve the free energy of the system as the potential decays by transferring energy to the distribution. **This transfer of energy from electrostatic potential fluctuations to the perturbed distribution is Landau damping**[6]. The results of the transfer is the formation of small scale structure in the distribution as a function of velocity scale. This shearing is illustrated at two times (early and late) for a simple system in Fig.9. Eventually the small scale structure gets small enough, and even an minuscule level of collisionality will act to smooth out the distribution.

II.3.1. *Some Actual Calculations*

After having patiently sat through the above mathematical manipulations, let's turn to some more quantitative calculations with more practical applications. For instance, how quickly does Landau damping actually damp a wave? To answer that, we will have to start making some assumptions, such as that the background distribution is a Maxwellian

$$F_s = \frac{n_{0s}}{\pi^{3/2} w_s^3} \exp\left(\frac{-v^2}{w_s^2}\right) \tag{II.33}$$

[6]The problem set has an alternative derivation that may be more physically intuitive

where the thermal velocity is defined $w_s \equiv \sqrt{2T_{0s}/m_s}$. Let's solve $D(\omega, \boldsymbol{k}) = 0$ (see Eqn. II.25).

$$\begin{aligned} D(\omega, \boldsymbol{k}) &= \sum_s \frac{4\pi}{k^2}\frac{q_s^2}{m_s}\int d^3\boldsymbol{v}\frac{-2\boldsymbol{k}\cdot\boldsymbol{v}}{w_s^2}\frac{F_s}{\omega - \boldsymbol{k}\cdot\boldsymbol{v}} \\ &= \sum_s \frac{4\pi q_s^2 n_{0s}}{k^2 T_{0s}}\int_0^\infty \frac{dv_\perp^2}{w_s^2}\exp\left(-\frac{v_\perp^2}{w_s^2}\right)\int_0^\infty \frac{dv_\parallel}{\sqrt{\pi}w_s}\frac{\exp\left(-\frac{v_\parallel^2}{w_s^2}\right)v_\parallel}{v_\parallel - \omega/k_\parallel} \\ &= \sum_s \frac{4\pi q_s^2 n_{0s}}{k^2 T_{0s}}\left[1 + \xi_s Z(\xi_s)\right] = 0. \end{aligned} \tag{II.34}$$

The plasma dispersion function

$$Z(\xi) = \pi^{-1/2}\int_{-\infty}^{\infty}\frac{dt\exp\left(-t^2\right)}{t-\xi} \tag{II.35}$$

with argument $\xi_s = \omega/k_\parallel w_s$ is a frequently employed function in plasma physics . Many of its features and limits are discussed in Fried & Conte (1961), and the most useful ones can be found in the NRL Plasma Formulary. One useful feature of Z is that for $\xi_s \ll 1$, $Z(\xi_s) \approx i\sqrt{\pi}$. Also, we can use the large difference in ion and electron masses ($m_p \approx 1836 m_e$) to write $\xi_e \sim \xi_i\sqrt{m_e/m_i} \ll \xi_i$, effectivitly eliminating $\xi_e Z(\xi_e) \ll 1$ from Eqn. II.35, which can be simply expressed as

$$\xi_i Z(\xi_i) = -(1+\tau) \tag{II.36}$$

where $\tau \equiv (q_e/q_i)(T_{0i}/T_{0s})$. This is the ion-acoustic wave dispersion relation. These waves experience Landau damping. Let's characterize that damping.

We consider the case where $|\xi_i| \gg 1$ (or $\omega >> k_\parallel w_i$) and for weak damping $(\gamma/\omega) << 1$. In this limit,

$$\xi_i Z(\xi_i) \approx i\sqrt{\pi}\xi_i e^{-\xi_i^2} - 1 - \frac{1}{2\xi_i^2} + \mathcal{O}(\frac{1}{\xi_i^4}). \tag{II.37}$$

Using this limit, Eqn.II.36 becomes

$$i\sqrt{\pi}\xi_i e^{-\xi_i^2} - \frac{1}{2\xi_i^2} = -\tau. \tag{II.38}$$

This can be separated into real and imaginary components, which after some manipulation yields a real frequency

$$\omega = |k_\parallel|\sqrt{\frac{T_e}{m_i}} \tag{II.39}$$

and a damping rate

$$\gamma = -|k_\parallel| w_i \sqrt{\pi} e^{-\xi_i^2}\xi_i^4. \tag{II.40}$$

To ensure a posteriori that $(\gamma/\omega) << 1$, we take calculate the ratio

$$\frac{\gamma}{\omega} = -\sqrt{\pi}\left(\frac{T_e}{2T_i}\right)^{3/2}\exp\left(-\frac{T_e}{2T_i}\right), \tag{II.41}$$

and find that our solution is consistent with our assumptions as long as $T_e \gg T_i$. This is the Landau damping rate of an ion-acoustic wave.

So, what is happening here? There are some particles that have speeds $v_\parallel \sim \omega/k_\parallel$. For the case of Landau damping, left panel of Fig. 10, there are more particles slightly slower

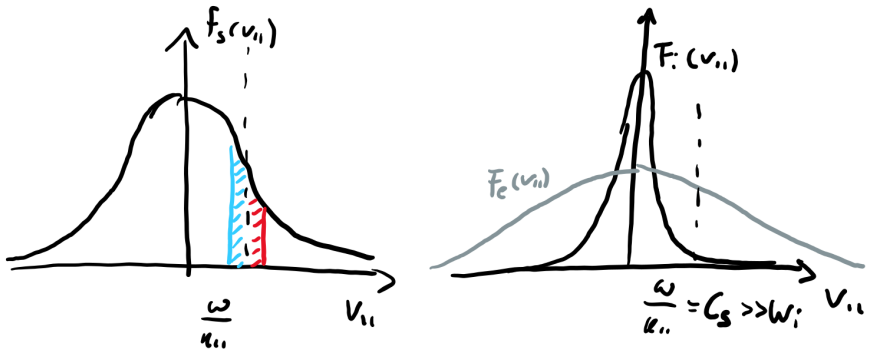

FIGURE 10. Distribution

than the resonant velocity than slightly faster (look ahead to the next lecture for the case of resonant instabilities). The lagging particles will see a stationary electric field in their reference frame and be accelerated; the leading particle will also see a stationary field, but be decelerated. As there are more particles gaining energy than losing energy, the wave damps, eventually flattening the distribution near the resonant velocity. A quantitative treatment of such flattening must be tackled with quasilinear theory, a topic beyond the scope of this lecture.

The more particles near the resonant velocity, the stronger the damping. This is why Landau damping is relatively weak in the case of $T_i/T_e \ll 1$ (right panel of Fig. 10); for a cold proton distribution with $c_s \ll w_i$, there are few particles that can act to damp the wave. For a hotter distribution of protons, with $c_s \sim w_i$, the damping can be much, much stronger.

For those more interested in the details (and more topics than an hour can afford) consider reviewing notes by Alex Schekochihin
http://www-thphys.physics.ox.ac.uk/people/AlexanderSchekochihin/KT/2015/KTLectureNotes.pdf
from which some of this material was extracted.

Takeaway Points:

- When collisions are insufficiently strong to enforce fluid-like behavior, phenomena associated with the velocity distribution of particles arise.
- The cannonical collisionless phenomenon is Landau damping, a transfer of energy from electrostatic waves to the particle distribution via a wave-particle resonance. This transfer leads to the formation of small scale structure in the velocity distribution.
- The strength of the damping is dependent on the number of particles near the resonant velocity, and the slope of the velocity distribution at that same point.
- A refresher on complex analysis is useful for working through plasma kinetic theory.

PART III

Linear theory of kinetic instabilities: Bumps, Beams, and Anisotropies

III.1. Kinetic Instabilities

While the Vlasov equation neglects collisions which act to move the plasma system towards a lower energy state, other mechanisms are retained that can perform that role in moving the system toward thermodynamic equilibrium. These mechanisms are call instabilities. Instabilities cause an initial small perturbation to grow, rather than damp, with time. In this lecture we will focus on the how departures from thermodynamic equilibrium in the velocity distribution of the constituent species, $f_s(\boldsymbol{x}, \boldsymbol{v}, t)$, rather than cases discussed by Prof. Kunz where there is free energy available in the structure of the system purely in configuration space (e.g. the Kelvin Helmholtz instability).

III.1.1. *General Stability Considerations*

We start somewhat more abstractly, asking if there are conditions under which stability can be guaranteed.

We return to the ground work laid out in the previous lecture, where we wrote that solutions that satisfy

$$D(\omega, \boldsymbol{k}) = 1 - \sum_s \frac{4\pi}{k^2} \frac{q_s^2}{m_s} \int d^3\boldsymbol{v} \frac{\boldsymbol{k} \cdot \partial F_s / \partial \boldsymbol{v}}{(\omega - \boldsymbol{k} \cdot \boldsymbol{v})} = 0 \tag{III.1}$$

are the normal mode solutions for the electrostatic Vlasov-Poisson system.[7]

We will consider the case of a monotonically decreasing function F_s, and assume that there exists an unstable solution, that is that $\gamma = \mathcal{I}(\omega) > 0$. We define $\omega_r = \mathcal{R}(\omega)$.

One can separate $D(\omega, \boldsymbol{k}) = 0$ into its real and imaginary components, which must separately satisfy the equality:

$$D_r = 1 - \frac{4\pi}{k^2} \frac{q_s^2}{m_s} \int_{-\infty}^{\infty} dv \frac{v \partial F / \partial v}{\left(v - \omega_r/|k|\right)^2 + \gamma^2/k^2} = 0 \tag{III.2}$$

$$D_i = \int_{-\infty}^{\infty} dv \frac{\partial F / \partial v}{\left(v - \omega_r/|k|\right)^2 + \gamma^2/k^2} = 0 \tag{III.3}$$

Importantly for a monotonically decreasing function, $v \partial F / \partial v \leqslant 0$ for all v, and therefore the integral in Eqn III.3 cannot be satisfied for all $\gamma > 0$. This statement is know as Gardner's Theorem: If a distribution decreases monotonically away from its maximum, the distribution is stable. Importantly, this does not depend on the frame of reference selected. As long as there exists a frame for which F is monotonically decreasing, F is stable.

III.1.2. *Two-Stream Instability*

So, a single monotonically decreasing function can't be unstable. The next obvious case to try is two functions. They can't have overlapping maxima, otherwise they would add up to a single monotonically decreasing function. Such a system of two separate populations is typically referred to as a two-stream system when the populations are of

[7] Eqn II.25 dropped the factor of 1 due to the low-frequency approximation assumed in the enforcement of quasineutrality.

similar amplitude, or a bump-on-tail (or beam and core) distribution when one population is much smaller.

Let's start with the two-stream case, with a ion beam moving relative to the electrons. For simplicity, treat the distributions as delta functions:

$$F_i = \delta\left(v - \frac{\boldsymbol{k}\cdot\boldsymbol{V}_0}{|k|}\right) \tag{III.4}$$

$$F_e = \delta\left(v\right). \tag{III.5}$$

This makes the integrals in D trivial, resulting in

$$1 = \frac{\omega_{pe}^2}{\omega^2} + \frac{\omega_{pi}^2}{\left(\boldsymbol{k}\cdot\boldsymbol{V}_0 - \omega\right)^2} \tag{III.6}$$

with the plasma frequency defined as $\omega_{ps}^2 = 4\pi n_s q_s^2/m_s$.

Plotting the right hand side of Eqn III.6 in **Figure 9.3.1**, we see real roots given by the intersection of the functional curve with 1. When the minimum of the curve is above 1, we have two real and two imaginary solutions, one of the later is the unstable mode. One can determine that this minimum arises at

$$\omega_A = \boldsymbol{k}\cdot\boldsymbol{V}_0\left[\frac{\left(\omega_{pe}/\omega_{pi}\right)^2}{\left(\omega_{pe}/\omega_{pi}\right)^{2/3}+1}\right] \tag{III.7}$$

and that the condition for the right hand side of Eqn III.6 to be greater than 1 at ω_A is

$$|\boldsymbol{k}\cdot\boldsymbol{V}_0| < \omega_{pe}\left[1+\left(\frac{\omega_{pi}}{\omega_{pe}}\right)^{2/3}\right]^{3/2}. \tag{III.8}$$

We could have equally well looked at the case of two electron beams, or two ion beams, as no sign of the charge of the species was included in the analysis. Importantly, this calculation begins to break down when the effects of a realistic, finite width velocity distribution are properly accounted for; what we have done thus far is valid as long as

$$|\frac{\boldsymbol{k}\cdot\boldsymbol{V}}{k} - \frac{\omega}{k}| \gg w_i \text{ and } V_0 \gg w_e. \tag{III.9}$$

The fastest growing mode arises for

$$\omega \approx \omega_{pe}\left[1 + i\frac{\sqrt{3}}{2}\left(\frac{m_e}{2m_i}\right)^{1/3}\right]. \tag{III.10}$$

What is driving this instability? A straightforward interpretation is that of charge bunching. A local increase in the density of the electrons induces a change perturbation in a stream that passes over the bunch. Electrons passing over the bunch will be slowed down, and that slowing down will produce an increase in the local electron density, reinforcing the original clump. Thus an instability is formed.

III.1.3. *Bump-on-Tail Instability*

As was hinted at in the previous section, we need to develop a means of handling the effects of the thermal spread in velocity (the kinetic effects).

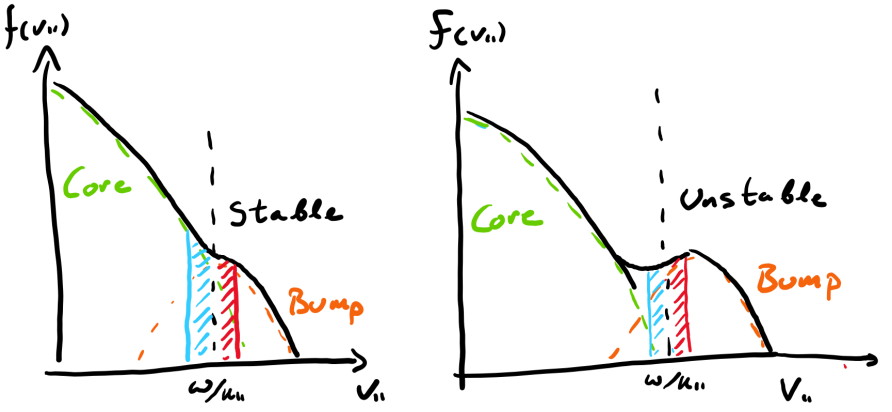

FIGURE 11. Two cases of the Bump-on-Tail distribution, one in which the beam is not sufficiently dense, cold, or fast to drive unstable waves (left) and one where a resonant instability occurs.

As a tractable test case, we consider the bump-on-tail distribution

$$\begin{aligned} F_e =& \frac{n_1}{n_e}\left(\frac{1}{w_{e1}}\right)^{3/2}\exp\left(-\frac{v^2}{w_{e1}}\right)+\frac{n_2}{n_e}\delta(v_x)\delta(v_y)\frac{1}{\sqrt{w_{e2}}} \\ &\times\frac{1}{2}\left\{\exp\left[-\frac{(v_z-V_0)^2}{w_{e2}^2}\right]+\exp\left[-\frac{(v_z+V_0)^2}{w_{e2}^2}\right]\right\} \end{aligned} \tag{III.11}$$

An analytic dispersion relation for a plasma with this distribution requires the use of the *Weak Growth Approximation*, where we will assume $\gamma \ll \omega$. Under this assumption, one can Taylor expand $D(\omega = (\omega_r, \gamma))$ about ω_0

$$\begin{aligned} D(\omega) &= D(\omega_0)+\gamma\frac{\partial D(\omega_0)}{\partial\omega}+... \\ D(\omega) &= D(\omega_0)+\gamma\frac{\partial\omega_r}{\partial\omega}\frac{\partial D(\omega_0)}{\partial\omega_r}+\gamma\frac{\partial\gamma}{\partial\omega}\frac{\partial D(\omega_0)}{\partial\gamma}+... \\ D(\omega) &= D(\omega_0)+i\gamma\frac{\partial D(\omega_0)}{\partial\omega_r}. \end{aligned} \tag{III.12}$$

Splitting D into its real and imaginary components, D_r and D_i (see Eqn. III.3 for the general expressions), we can write (again, assuming $\gamma \ll \omega$)

$$D_r(\omega) = 0 \tag{III.13}$$

$$D_i(\omega)+\gamma\frac{\partial D_r(\omega_0)}{\partial\omega_r}=0. \tag{III.14}$$

Manipulation of the imaginary component yields an expression for the growth rate

$$\gamma = \frac{-D_i(\omega)}{\frac{\partial D_r(\omega_0)}{\partial\omega_r}}. \tag{III.15}$$

Under the assumption that the wave phase speed is large compared to the thermal velocity $\omega/|k| \gg w_e$, and that $n_1 \gg n_2$, the real part of the frequency can be found

$$\omega_r^2 \approx \omega_{pe}^2\left(1+3k^2\lambda_{D1}^2\right). \tag{III.16}$$

These frequencies are only very slightly different from those extracted from a single Maxwellian case. The imaginary component, however, can be quite different.

After some tedious algebra, one can find

$$\gamma \approx -\sqrt{\frac{\pi}{8}}\frac{\omega_{p1}}{k^3\lambda_{D1}^3}\exp\left(-\frac{1}{2k^2\lambda_{D1}^2}-\frac{3}{2}\right) + \frac{n_2}{n_1}\left(\frac{T_1}{T_2}\right)^{3/2}\frac{k^3}{k_z^3}\left(\frac{k_z V_0}{\omega_r}-1\right)\exp\left[-\frac{T_1/T2}{2k_z^2\lambda_{D1}^2}\left(1-\frac{k_z V_0}{\omega_r}\right)^2\right]. \tag{III.17}$$

The first term is just Landau damping associated with the core distribution. It will always damp, and never contribute to the growth of an unstable wave. The second term is from the bump, and only velocities satisfying $\omega_r/k_z = v$ will resonant (we assumed the beam was cold in the $\hat{x}$ and $\hat{y}$ directions). If a wave has a phase velocity smaller than V_0, the mean velocity of the bump distribution, it can contribute to an unstable mode. For velocities larger than V_0, the bump will contribute to the damping of already driven by the core distribution. For any value of v, the damping of growth of a wave is determined by the local slope of F_e; if the bump is large enough to force the total distribution to have a positive slope, the distribution will be unstable to waves with phase speeds matching ω_r/k_z.

By inspection, the destabilizing contribution from the bump is greatest at $|k_z V_0|/\omega = 1 + \sqrt{k_z^2\lambda_{D1}^2 T_2/T_1}$. Evaluating the for the maximum growth rate at that wavenumber yields

$$\gamma_{\max} = \sqrt{\frac{\pi}{8}}\frac{\omega_{p1}}{k^3\lambda_{D1}^3}\left[\frac{n_2}{n_1}\left(\frac{T_1}{T_2}\right)k^3\lambda_{D1}^3\frac{V_0^2}{w_{e1}^2}\exp\left(-\frac{1}{2}\right)-\exp\left(-\frac{1}{2k^2\lambda_{D1}^2}-\frac{3}{2}\right)\right]. \tag{III.18}$$

From this form, we see there are three ways to encourage unstable growth from the beam:

- Increase the number of beam particles (but not too much to invalidate the assumption $n_1 \gg n_2$).
- Make the beam more peaked (decrease T_2/T_1).
- Increase the bulk speed of the bump.

Generally, this kind of weak bump instability will always grow much more slowly than the two-stream instability.

III.1.4. *Nyquist Method and Penrose Criterion*

Can a more general means of determining the stability of a system be derived? In a word, yes.

We already have convinced ourselves that a monotonically decreasing, isotropic function is stable, and have identified two cases where departures from that ideal state lead to the growth of unstable modes.

In his time at Bell Labs, Nyquist developed a very general method for determining the stability of electric circuits against feedback(Nyquist 1932). Physicists aware of this method adopted it the systems of equations governing plasmas, and in time produced a simplified version (Penrose 1960).

This method depends on the fact that question of stability depends on determining if $D(\omega, \boldsymbol{k}) = 0$ has any solutions with $\mathcal{I}(\omega) = \gamma > 0$. If such solutions exist, then the system is unstable. Seizing on this mathematical statement, Nyquist stated that if one were to perform a contour integral of D^{-1} over the upper half complex plane, illustrated in red in the right hand panel of Fig. 12, the complex frequency solutions that satisfy $D(\omega, \boldsymbol{k}) = 0$ would be poles, and thus could be counted by an application of the residue theorem

$$\frac{1}{2\pi i}\oint\frac{d\omega}{D(\omega,\boldsymbol{k})}\frac{\partial D}{\partial\omega} = W_n \tag{III.19}$$

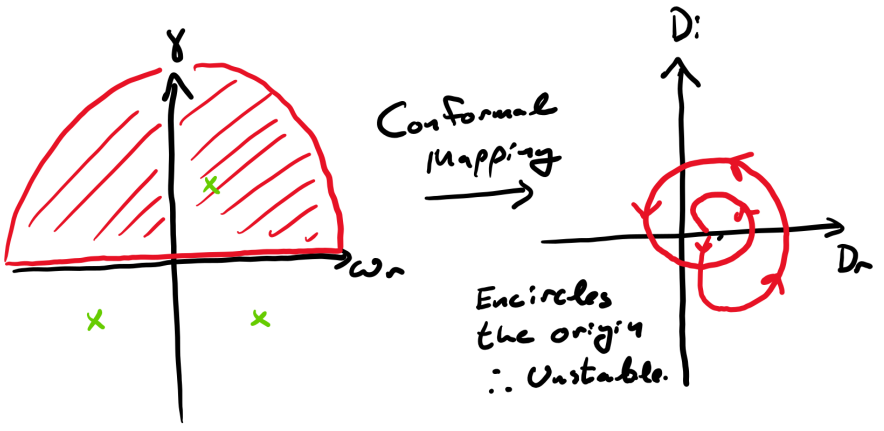

FIGURE 12. A schematic of the contour integral and the conformal mapping used to determine stability for the Nyquist method.

where W_n is the number of poles in the upper half complex plane, which corresponds to the number of unstable modes associated with the chosen plasma equilibrium, as the function $\frac{1}{D(\omega,\boldsymbol{k})}\frac{\partial D}{\partial \omega}$ has been constructed to have poles wherever D has zeros.

One way to visualize this integration is perform a conformal mapping of the value of $D(\omega)$ over the real ω axis from $\omega \to -\infty$ to $\omega \to \infty$. Such a mapping is illustrated in the right hand panel of Fig. 12. One can show, with sufficient patience or a reading of section 9.6 of Krall & Trivelpiece (1973), that the number of times this contour encircles the origin is equal to W_n.

As a simple example of this mapping, let's consider the case of a monotonically decreasing $F(v)$ with a peak at v_0, which we know to be stable. Returning to Eqn. III.3, we take advantage of the fact that $dH(x)/dy \equiv 0$ to rewrite the integral

$$\int_{-\infty}^{\infty} \frac{dF(v)/dv}{v-\omega/|k|}dv = \int_{-\infty}^{\infty} \frac{d\left[F(v)-F(\omega/|k|)\right]/dv}{v-\omega/|k|}dv. \tag{III.20}$$

We also will need to use the *Plemelj Relation* to simplify the imaginary component of D. This relation states

$$\lim_{\epsilon\to 0}\int_{-\infty}^{\infty} dx \frac{f(x)}{x-(x_0\pm i\epsilon)} = P\int_{-\infty}^{\infty} dx\frac{f(x)}{x-x_0} \pm i\pi f(x_0). \tag{III.21}$$

The real and imaginary components of the dielectric can thus be written, for real ω, ω, as

$$D_r = 1-\frac{\omega_{pe}}{k^2}\int_{-\infty}^{\infty} dv \frac{\partial F(v)-F(\omega/|k|)}{\left(v-\omega_r/|k|\right)^2} \tag{III.22}$$

$$D_i = -\pi\frac{\omega_{pe}^2}{k^2}\frac{\partial F}{\partial v}|_{v=\omega/|k|}. \tag{III.23}$$

From inspection, $D_i = 0$ for three values of ω, $-\infty, |k|v_0$. We can inspect the sign of D_r for these three frequencies. For $\omega = \pm\infty$, D_r is positive, with a value of 1 for $-\infty$ and $e^{2\pi i W_n}$ for ∞. At the peak v_0

$$D_r(\omega = |k|v_0) = 1+\frac{\omega_{pe}}{k^2}\int_{-\infty}^{\infty} dv \frac{\partial F(v_0)-F(v)}{\left(v-\omega_r/|k|\right)^2} > 0. \tag{III.24}$$

This last inequality holds as F has a maximum at v_0, and thus $F(v_0) - F(v) \geqslant 0 \forall v$. Therefore, D_r is positive at all points where D_i vanishes, allowing us to construct the Nyquist diagram; see the bottom panel of Fig. 13. As the curve does not encircle the origin, there are no unstable modes.

Let's try a less trivial case, with a generic distribution with one minimum, at v_0, and two maxima, v_1 and v_2, with $F(v_1) > F(v_2)$. We can immediately write down the five frequencies at which D_i will be zero, $\omega = \pm\infty$, $|k|v_0$, $|k|v_1$, and $|k|v_2$. As before, we know that $D_r(\omega \to \pm\infty)$ and $D_r(\omega = |k|v_1)$ will be positive. The signs of D_r at the other two key frequencies will determine the stability of the plasma. While the exact values of D_r for $\omega = |k|v_0$ and $\omega = |k|v_2$ depend on the structure of F, we can state that $D_r(\omega = |k|v_0) < D_r(\omega = |k|v_2)$. More generally, if $D_r(\omega = |k|v) > 0$, the plasma is stable. This can be expressed mathematically as *the Penrose Criterion*:

$$P(F) = \int_{-\infty}^{\infty} \frac{F(v_0) - F(v)}{(v - v_0)^2} dv < 0. \tag{III.25}$$

If $P(F) < 0$, there must be some value of k for which $D_r(|k|u_2) > 0$ and $D_r(|k|u_0) < 0$. Even more usefully, the range of unstable wavevectors can be determined using

$$\omega_{pe}^2 \int_{-\infty}^{\infty} \frac{F(v_2) - F(v)}{(v - v_2)^2} dv < k^2 < \omega_{pe}^2 \int_{-\infty}^{\infty} \frac{F(v_0) - F(v)}{(v - v_0)^2} dv. \tag{III.26}$$

An important caveats: The Penrose criterion is a necessary and sufficient condition for *electrostatic* instabilities. It does not determine if *electromagnetic* waves can be driven. The more general Nyquist method can be used for both electrostatic and electromagnetic instabilities.[8]

Quoting Krall & Trivelpiece (1973)

> The Nyquist method is a powerful tool with which to study plasma stability because it makes it possible to predict stability by calculating the sign of D_r for a few particular values of ω_r rather than having to solve the equation $D = 0$.

III.1.4.1. *Weibel Instability*

Instead of being driven by multiple components, instabilities can also be driven by anisotropies in the velocity distribution.[9] The Weibel instability is such an example instability.

As a simple physical model, let's assume the ions are a fixed, immobile background and that the electrons are faster in the $\hat{y}$ direction; effectively $T_y > T_x$ or T_z; this system is sketched in Fig. 14. In this setup, there are equal numbers of forward and backward propagating in the hot ($\hat{y}$) direction, so there is no net current induced by the equilibrium distribution.

Let us now introduce a small magnetic fluctuation, rising from the noise, in the $\hat{z}$ direction. For simplicity, this small fluctuation will be sinusoidal $\delta B_z = B_z \sin(kx)$. This initially small fluctuation will perturb the motion of the electrons, via the $\boldsymbol{v} \times \boldsymbol{B}$ component of the Lorentz force. The initially straight paths of the electrons will be diverted, from the dashed to the solid lines in Fig. 14. These diversions of electrons will act to create streams of downward or upward moving electrons, depending on the phase of the δB_z fluctuation. Streams of charged particles produce a current $\boldsymbol{j} = q_e n_e \boldsymbol{v}_e$ in the $\pm\hat{y}$

[8] See Klein *et al.* (2017) for a discussion of an automated, numerical implementation of the Nyquist method.

[9] But what about Gardner? That proof by contradiction only applied to an monotonically decreasing, isotropic distribution. If the distribution is not isotropic, the plasma can be unstable.

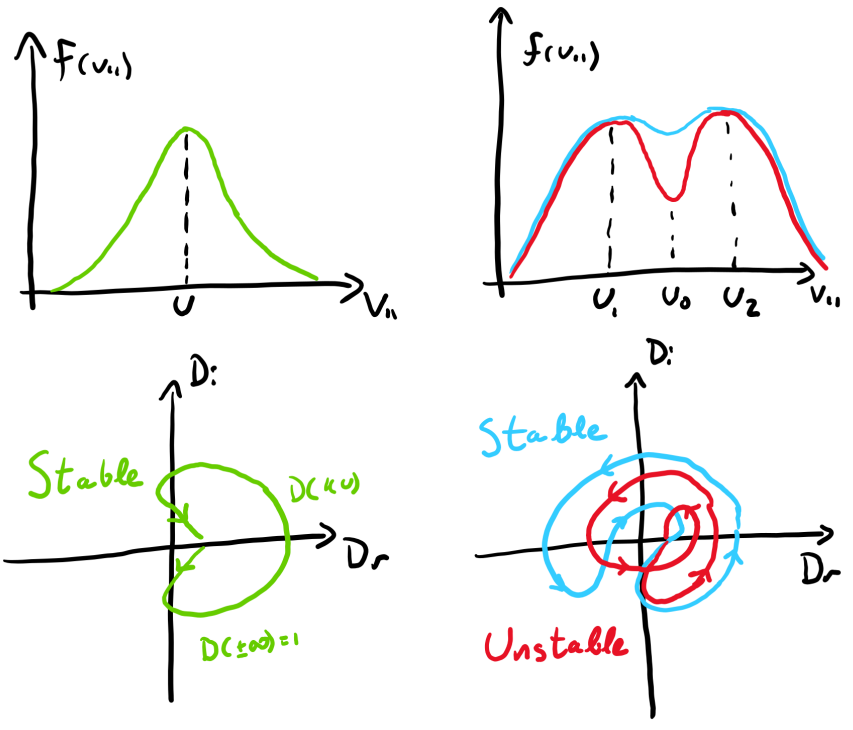

FIGURE 13. An application of the Nyquist method to a stable, monotonically decreasing function (left), as well as to a stable and unstable two-humped distribution.

direction. This current in turn reinforces the initial magnetic fluctuation, strengthening the Lorentz force and further enhancing the current channels.

An analogy can be drawn to the two stream instability, but instead of electrostatic perturbations reinforced by spatial bunches of charge, electromagnetic perturbations are reinforced by filaments of current.

Unsurprisingly, this problem can be treated in a much more sophisticated fashion. We leave the maths to the enterprising student[10] and state by fiat that a linearization of electromagnetic fluctuations in an electrostatic systems

$$\frac{\partial \delta f_s}{\partial t} + i\boldsymbol{k}\cdot\boldsymbol{v}\delta f_s + \frac{q_s}{m_s}\left(\delta\boldsymbol{E} + \frac{\boldsymbol{v}\times\boldsymbol{B}}{c}\right)\cdot\frac{\partial F_s(\boldsymbol{v})}{\partial \boldsymbol{v}} = 0 \tag{III.27}$$

combined with a bi-Maxwellian distribution of electrons

$$F_e = \frac{n_{0s}}{\pi^{3/2} w_{\parallel,e} w_{\perp,e}^2}\exp\left(-\frac{v^2}{w_{\parallel,e'}^2} - \frac{v^2}{w_{\perp,e'}^2}\right) \tag{III.28}$$

yields a growth rate of

$$\gamma = \frac{k w_{\parallel,e}}{\sqrt{\pi}}\frac{T_{\parallel,e}}{T_{\perp,e}}\left(\frac{T_{\perp,e}}{T_{\parallel,e}} - 1 - k^2 d_e^2\right). \tag{III.29}$$

[10] Questions 2 and 3 from the Plasma Kinetics Problem set found in http://www-thphys.physics.ox.ac.uk/people/AlexanderSchekochihin/KT/2015/KTLectureNotes.pdf can help to guide this derivation.

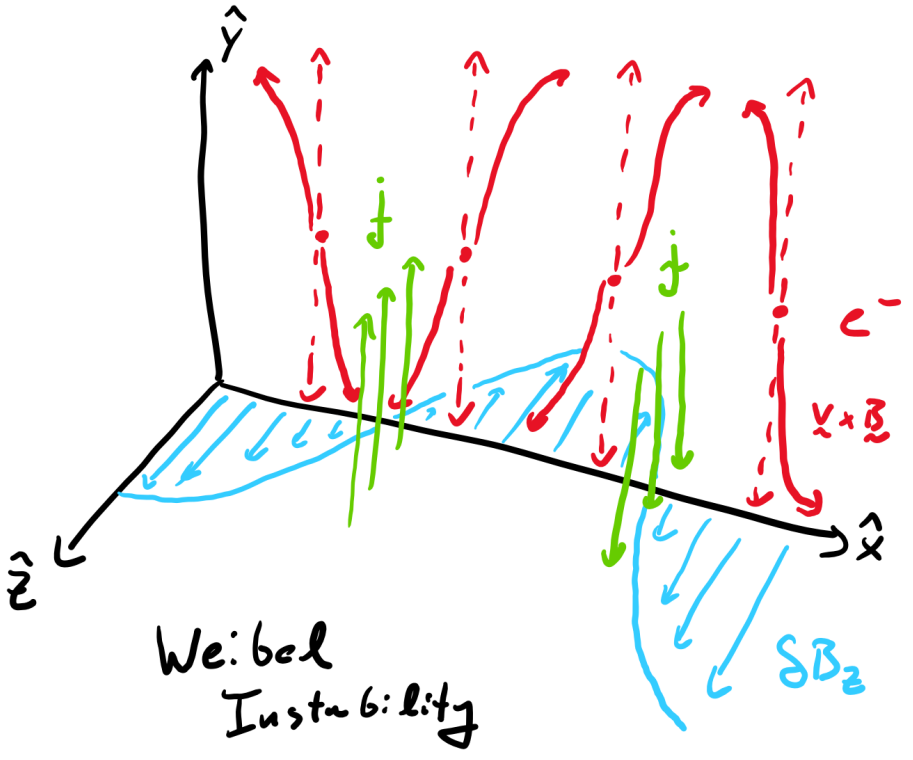

FIGURE 14. A schematic of the Weibel instability.

The Weibel instability is commonly invoked to arise in astrophysical plasma systems, including in collisionless shocks around supernova remnants and magnetogenesis.

III.1.4.2. *Other Kinetic Instabilities*

There are a plethora of other kinds of kinetic instabilities that can arise in collisionless or weakly-collisional magnetized plasma systems. Some examples are the Alfvén Ion Cyclotron instability, which depends on the cyclotron rather than the Landau resonance, the mirror instability, which is driven by a difference in the response of particles with $v_\parallel \approx 0$ and the rest of the distribution to magnetic field fluctuations, and a family of fire-hose instabilities (fluid (Chew *et al.* 1956), parallel, and obliqueHellinger & Matsumoto (2000)), which depend on the presence of an excess parallel pressure. Details on most of these can be found in the excellent Gary (1993), with updates in Klein & Howes (2015) and Yoon (2017), or the table in Verscharen *et al.* (2019). The presence of the action of these instabilities in governing the evolution of the solar wind can be inferred from statistical observations (Kasper *et al.* 2002; Bale *et al.* 2009) as well as measurements of wavestorms (Jian *et al.* 2014; Wicks *et al.* 2016; Gary *et al.* 2016).

Takeaway Points:

•Departures from a Maxwellian velocity space distribution is a source of free energy that can, under certain circumstances, lead the generation of waves that act to move the system toward Maxwellianity.

- Typical features that can drive instabilities are beams (either cold or hot) or anisotropies in the velocity distribution.
- A number of tools are available to determine the stability of a system. Most require some familiarity with complex analysis.
- The wave modes associated with these instabilities are frequently observed in weakly collisional systems.

REFERENCES

Bale, S. D., Kasper, J. C., Howes, G. G., Quataert, E., Salem, C. & Sundkvist, D. 2009 Magnetic Fluctuation Power Near Proton Temperature Anisotropy Instability Thresholds in the Solar Wind. *Phys. Rev. Lett.* **103** (21), 211101.

Belcher, J. W. & Davis, Jr., L. 1971 Large-amplitude Alfvén waves in the interplanetary medium, 2. *J. Geophys. Res.* **76**, 3534.

Bender, C. M. & Orszag, S. A. 1978 *Advanced Mathematical Methods for Scientists and Engineers*.

Brown, J.W. & Churchill, R.V. 2004 *Complex Variables and Applications*. McGraw-Hill Higher Education.

Chew, G. F., Goldberger, M. L. & Low, F. E. 1956 The Boltzmann Equation and the One-Fluid Hydromagnetic Equations in the Absence of Particle Collisions. *Royal Society of London Proceedings Series A* **236**, 112–118.

Fried, B. D. & Conte, S. D. 1961 *The Plasma Dispersion Function*. Academic Press.

Gary, S. P. 1993 *Theory of Space Plasma Microinstabilities*.

Gary, S. P., Jian, L. K., Broiles, T. W., Stevens, M. L., Podesta, J. J. & Kasper, J. C. 2016 Ion-driven instabilities in the solar wind: Wind observations of 19 March 2005. *J. Geophys. Res.* **121**, 30–41.

Hellinger, P. & Matsumoto, H. 2000 New kinetic instability: Oblique Alfvén fire hose. *J. Geophys. Res.* **105**, 10519–10526.

Jian, L. K., Wei, H. Y., Russell, C. T., Luhmann, J. G., Klecker, B., Omidi, N., Isenberg, P. A., Goldstein, M. L., Figueroa-Viñas, A. & Blanco-Cano, X. 2014 Electromagnetic Waves near the Proton Cyclotron Frequency: STEREO Observations. *Astrophys. J.* **786** (2), 123.

Kasper, J. C., Lazarus, A. J. & Gary, S. P. 2002 Wind/SWE observations of firehose constraint on solar wind proton temperature anisotropy. *Geophys. Res. Lett.* **29** (17), 1839.

Klein, K. G. & Howes, G. G. 2015 Predicted impacts of proton temperature anisotropy on solar wind turbulence. *Phys. Plasmas* **22** (3), 032903.

Klein, Kristopher G., Kasper, Justin C., Korreck, K. E. & Stevens, Michael L. 2017 Applying Nyquist's method for stability determination to solar wind observations. *Journal of Geophysical Research (Space Physics)* **122**, 9815–9823.

Krall, N. A. & Trivelpiece, A. W. 1973 *Principles of plasma physics*. McGraw-Hill.

Landau, L. D. 1946 On the vibrations of the electronic plasma. *J. Phys.(USSR)* **10**, 25–34, [Zh. Eksp. Teor. Fiz.16,574(1946)].

Nicholson, D.R. 1983 *Introduction to plasma theory*. Wiley.

Nyquist, Harry 1932 Regeneration theory. *Bell system technical journal* **11** (1), 126–147.

Penrose, O. 1960 Electrostatic Instabilities of a Uniform Non-Maxwellian Plasma. *Physics of Fluids* **3**, 258–265.

Verscharen, Daniel, Klein, Kristopher G. & Maruca, Bennett A. 2019 The multi-scale nature of the solar wind. *arXiv e-prints* p. arXiv:1902.03448.

Vlasov, AA 1945 Theory of vibrational properties of electron gas and its applications. *J. Phys.(USSR)* **9**, 25.

Wicks, R. T., Alexander, R. L., Stevens, M., Wilson, L. B., III, Moya, P. S., Viñas, A., Jian, L. K., Roberts, D. A., O'Modhrain, S. & Gilbert, J. A. 2016 A Proton-cyclotron Wave Storm Generated by Unstable Proton Distribution Functions in the Solar Wind. *Astrophys. J.* **819** (1), 6.

Yoon, Peter H. 2017 Kinetic instabilities in the solar wind driven by temperature anisotropies. *Reviews of Modern Plasma Physics* **1**, 4.